



Fleet scheduling for electric towing of aircraft under limited airport energy capacity

M. Zoutendijk^{a,*}, M. Mitici^b

^a Delft University of Technology, Kluyverweg 1, 2629 HS, Delft, The Netherlands

^b Utrecht University, Heidelberglaan 8, 3584 CS, Utrecht, The Netherlands

ARTICLE INFO

Keywords:

Electric taxiing
Electricity capacity
Fleet scheduling
Adaptive Large Neighbourhood Search
Charging strategy

ABSTRACT

Taxiing aircraft using electric vehicles is seen as an effective solution to meet aviation targets of climate neutrality. However, making the transition to electric taxiing operations is expected to significantly increase the electricity demand at airports. In this paper we propose a mixed-integer linear program to schedule electric vehicles for aircraft towing and battery charging, while considering a limit for the supply of energy. The objective of the schedule is to maximize emissions savings. For computational tractability, we develop an Adaptive Large Neighbourhood Search which makes use of multiple local search heuristics to identify scheduling solutions. For daily scheduling with a small fleet size, the developed heuristic achieves solutions with an average 4% gap to the best linear programming solution. The results show that charging the vehicles during daytime is essential to maximize saved emissions: removing charging opportunities for a few hours during the day reduces the performance by an average of 6.4%. In addition, it is found that fast charging leads to low vehicle downtime, unless the battery size exceeds 750kWh, when charging rates over 150kW become unnecessary. Overall, our model provides support for infrastructure planning of airports during the transition to aircraft electric taxiing.

1. Introduction

The aerospace industry has committed to reducing net greenhouse gas emissions to zero in the USA and to 10% of 1990 emissions in the EU by 2050 [1,2]. In addition to emissions produced while flying, the aerospace industry also produces ground-based emissions. Electric taxiing is a promising technique for reducing these emissions. In this work, the focus is on external electric taxi systems, where an electric towing vehicle (ETV) tows aircraft from gates to runways and vice versa. Electric towing vehicles are currently operational at several airports, and are under further development [3]. Their implementation is expected to reduce taxiing fuel use by up to 80% [4] and thus reduce the airport emissions of greenhouse gases [5]. This is not only beneficial for the emission goals of airlines, but also improves air quality and reduces noise pollution for airport personnel, passengers and residents of airport surroundings [6].

The technical feasibility of the external ETS has been investigated in literature, and shown during early implementation. The next step is to move towards large scale implementation, and to find out how many towing vehicles are needed for seamless surface movement. This requires airport infrastructural planning and a strategy for operational management of large fleets. Vehicle operation needs to be scheduled,

taking into account airport routing, flight schedules and electricity use. A model is needed that creates a daily towing schedule for ETVs to aircraft. Such a model can be used by airport operators to manage current or future ETV fleets at airports, and also by airport planners to consider the infrastructural requirements needed. Below we review existing studies addressing comparable problems in other domains.

Vehicle fleet scheduling

Many studies have developed models to optimize schedules for a fleet of vehicles to perform certain tasks. Bunte and Kliever [7] provide an overview of modelling approaches and solution strategies from literature for the vehicle scheduling problem: every vehicle in a fleet performs a sequence of tasks, and all tasks are covered once. Extensions to this problem can be the existence of multiple vehicle depots, vehicle types and time windows. The discussed works aim to minimize fleet size and/or operational costs. Hoff et al. [8] provide a similar overview, focusing on the fleet size and mix vehicle routing problem, with many more possible extensions. Recent examples of studies are: Rahman and Nielsen [9], who employ a Mixed-Integer Linear Programming (MILP) model, a Genetic Algorithm and an iterated greedy model for scheduling automated transport vehicles. The results show that the

* Corresponding author.

E-mail address: M.Zoutendijk@tudelft.nl (M. Zoutendijk).

use of the heuristics can increase the utilization of vehicle capacity and allows for near real-time scheduling of tasks. Alizadeh Foroutan et al. [10] consider both the routing and the scheduling problem for a capacitated fixed-size mixed fleet, and aim to minimize CO₂ emissions. A Simulated Annealing and Genetic Algorithm formulation proved to be able to find near-optimal solutions for medium and large-sized problem instances. Ganji et al. [11] consider a capacitated mixed fleet problem with time windows and multiple objectives; minimizing distribution costs, fuel, emissions and delivery tardiness. The authors use Particle Swarm Optimization, Ant Colony Optimization and Genetic Algorithms to solve the problem, where the latter showed the best performance. Andrade-Michel et al. [12] consider the problem of bus driver scheduling, minimizing the number of buses that cannot be assigned a driver. The authors compare an MILP approach to a variable neighbourhood search, and include stochastic simulations of driver absenteeism. Comparisons to regular models that do not simulate driver absenteeism show a decrease in operating costs and in driver swaps.

An increasing amount of studies is focusing on scheduling generic electric vehicles (EVs) for operations and charging. Hiermann et al. [13] consider a routing problem with a mixed fleet of EVs, where vehicles are assigned to customers with time windows. They optimize for the best fleet composition, choices of recharging moments and locations. Routing is done using labelling algorithms, and scheduling using branch-and-price and a heuristic based on Adaptive Large Neighbourhood Search (ALNS). Schiffer and Walther [14] solve an MILP-formulated location routing problem to find charging station locations, while optimizing for travelling distance, fleet size and number of stations. Keskin and Çatay [15] apply ALNS to schedule EV tasks with time windows, and allow partial recharging. In addition to customer removal and insertion algorithms, the authors also introduce removal and insertion algorithms for visits to charging stations. Emde et al. [16] develop heuristics to schedule a fleet of EVs performing round trips including recharging breaks. They aim to minimize the fleet size and maximize fairness in workload for EV operators. Their neighbourhood search heuristic based on operations 'push' and 'swap' performs best and can solve problem instances in a few minutes. Frey et al. [17] solve a vehicle routing and scheduling problem with customer time windows. In addition to a branch-price-and-cut algorithm introduced in earlier work, they introduce an ALNS approach. Their approach allows moving to infeasible solutions, and penalizes such solutions in the objective function. Several special removal operators based on the spatial arrangement of customer locations are introduced. Last, Foda et al. [18] develop a generic optimization model for electric bus fleets, with a very broad approach, taking into account a mixture of multiple objectives. Since the authors infer that all system parameters should be included in the model as system parameters, their model outputs include charging schedules, but also battery properties and optimal charging infrastructure parameters.

Fleet scheduling approaches for electric taxiing vehicles

In recent years, several authors have started to research the routing and scheduling challenges connected to ETV implementation. An important difference between EV and ETV scheduling is the split between driving and towing: the speed, road usage, conflict avoidance and time constraints are different when driving an ETV compared to towing an aircraft. These aspects introduce additional constraints and complications that need to be taken into account when creating a realistic model of airport surface movement with electric taxiing.

One of the first works concerning ETV scheduling is van Baaren and Rolling [19], who create an MILP model minimizing fuel consumption. The model generates trips that can be performed on one battery charge. The model is applied to two airports. The fuel savings and electricity costs are calculated, and the minimum fleet size is ascertained. Soltani et al. [20] develop an MILP model to assign diesel-powered towing vehicles to 205 aircraft, and introduce extra variables and constraints to ensure conflict and collision avoidance, while minimizing the sum

of taxiing delay costs, maintenance costs and labour costs. It is found that the optimal number of vehicles for Montreal-Trudeau International Airport (CYUL) is 12, reducing taxiing fuel consumption by 95%. Salihi et al. [21] develop a discrete event simulation for scheduling a year of ETV operation, with the goal of modelling the taxiway congestion that can be expected from using electric taxiing. The taxi routes are calculated in advance. It is assumed that all charging can be done during the night. It is found that electric taxiing leads to a longer taxiing time, as the ETVs taxi slower than the aircraft, and the aircraft have to wait after requesting an ETV. Building on earlier work, Zaninotto et al. [22] create a real-time simulation to schedule ETVs to aircraft. Conflict avoidance is performed by slightly delaying aircraft (less than 3 min) where necessary, before selecting the ETV. The model minimizes taxiing delays and route lengths. The ETV state of charge and recharging are considered throughout the simulation. More than 80% of flights were assigned to an ETV, with a fleet size of 25% of the airfield hourly traffic. The tow truck utilization time was 30%. Also building on their earlier work, van Oosterom et al. [23] develop an MILP and a greedy model to dispatch multiple types of ETVs to aircraft. Deciding which ETVs charges when is based on the residual state-of-charge of the ETVs. The objective of the models is to minimize the fleet size required to tow all flights in the daily flight schedule. A 5% optimality gap is obtained by the greedy model compared to the MILP approach. Applying both models in a rolling horizon approach and using a flight schedule including historical flight delays, the authors show that 95% of flights can still be towed by ETVs. Last, Ahmadi and Akgunduz [24] develop a 1 h rolling horizon MILP model with the goal of showing the best fleet size to be purchased by airports. The model minimizes taxiing delay, total taxiing time and fuel consumption. Aircraft can either be towed or taxi in the regular way. The rolling horizon approach allows for solving realistic size problems in foreseeable time, and accommodating for flight disruption during the day. The model does not consider charging stations and charging times.

Transport electrification at airports

The transport industry has far-reaching ambitions for electrification, e.g. the EU will only allow zero-emission vehicles from 2035 onwards [25]. There has been research interest into the electrical infrastructure requirements to meet such ambitions.

Some authors investigate the option of supplying the electrical grid with energy from idle EVs, i.e. electric vehicle-to-grid delivery, such as Mahmud et al. [26] and Li et al. [27]. In a review paper, Uddin et al. [28] identify this as one of the three major strategies considered in literature for peak load shaving, along with demand side management, and making use of energy storage systems (ESS). However, rather than using EV charge to mitigate demand peaks, such peaks can also occur when charging these EVs. Solutions suggested in literature include ESSs, battery swapping [29] and time-based electricity pricing [30]. Generally, it is expected that the electricity demand will form a temporary bottleneck for certain electrification developments. For example, Forrest et al. [31], a large scale study of energy infrastructure requirements for EVs in California, find that smart charging technology such as V2G and smart energy storage facilities can help provide in energy demands at off-peak hours. However, they stress that such techniques would still require a large excess of renewable energy generation in the first place. Moon et al. [32] estimate future electricity demand due to EVs in South Korea and determine where and at which time demand peaks will appear. They predict that current power grid infrastructure in parts of the country may not be able to cover the predicted demand.

The electricity demand at airports without considering transport electrification stems mainly from HVAC systems and lighting, report [33], who describe the main airport energy sources and consumers, and suggest ways to reduce electricity consumption at airports. Uysal and Sogut [34] apply a holistic architecture-based approach to airport energy demand and report large potential savings for light and thermal management in terminal buildings. In [35] energy demand patterns at

Santander Airport (LEXJ) are characterized and analysed on a daily and yearly basis, by studying their electrical load profiles. Current peak electricity demand for this medium-sized airport does not exceed 600 kW.

However, when accounting for transport electrification, more and more systems start to make their appeal on the airport electricity capacity. Electric vehicles charging at airport parking spaces, electrified ground support equipment [36], and electric aircraft [37] are all expected to contribute to the future electricity demand. Improving the electricity infrastructure or local power grid to keep up with these demands will take time. This suggests that it is wise to take into account that for a certain period the airport might only reserve limited electricity capacity for electric towing, while it is transitioning to sustainable airport surface movement.

In order to gain insight into the possibilities of electric taxiing under such circumstances, it is necessary to create a scheduling model that can adhere to electricity capacity constraints. The model should closely monitor state-of-charge of ETVs and decide when and where they are charged. The schedule created by this model should cover a full day of operation, to find the best schedule given specific daily electricity capacity profiles for ETV charging. In addition, to emulate realistic airport scenarios, the model should incorporate practical considerations such as a realistic airside airport model, ETV connecting/disconnecting times and conflict avoidance.

To the best of our knowledge, there is no previous work addressing the issue of *the effect of limited electricity capacity at airports* on the expected emission benefits of electric towing. In this paper we propose two models to assign ETVs to aircraft that take limited electricity capacity at airports into account. The main contributions of this paper are:

- We propose an MILP formulation for the ETV-to-aircraft assignment problem, that takes into account a limited electricity capacity at an airport. The model also tracks the state of charge and electricity demand of every ETV throughout the day, which is omitted in the majority of previous works.
- We propose an ALNS method including tailored removal/insertion heuristics to obtain time-efficient solutions of the full-day ETV-to-aircraft assignment problem.
- We apply our models for a large airport, and for various ETV electricity capacity profiles. We investigate the effects of having a limited electricity capacity on the ETV operations for these profiles.

The remainder of this paper is divided as follows: Section 2 introduces the ETV scheduling problem and the input data and parameters required. In Section 3 a model to calculate the emissions savings from the electric towing distance is described. Section 4 states the linear programming formulation describing the scheduling problem and Section 5 describes how this problem is solved using ALNS. Local search heuristics and notation for the ALNS algorithm are defined, as well as the local search framework. In Section 6 both models are applied to various instances of the ETV scheduling problem, to determine their efficacy, as well as the influence of ETV electricity capacity profiles and ETV battery properties on the results. Section 7 provides concluding remarks and future research directions.

2. Problem description and formulation

In this section the problem of scheduling ETVs to tow aircraft is defined, and the model developed to create the schedule is presented. The schedule consists of a *towing schedule* and a *charging schedule*. The former defines for each vehicle when it tows which aircraft, and the latter defines for each vehicle when and where it will be charged. An arriving or departing aircraft either performs regular taxiing (using the jet engines) or electric taxiing (being towed by an ETV). The ETVs tow aircraft, and charge at charging stations to replenish their

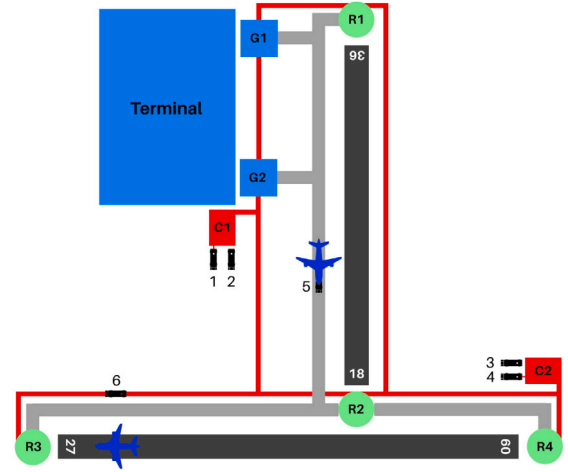


Fig. 1. Schematic overview of an example airport. Two runways are shown in black. Grey lines indicate taxiways (E^X) and thin red lines indicate service roads (E^S). Runway entry/exit points R1–R4 are indicated with green circles. Gate group nodes G1–2 are indicated with blue squares. Charging stations C1–2 are indicated with red rectangles. The airport traffic in this example consists of towing vehicles 1–6 and two aircraft.

battery. A limited amount of electricity capacity is assumed available at the airport for the charging of ETVs. The scheduling problem is therefore extended with constraints that track the electricity demand and capacity at discrete time steps. The problem is formulated as a Mixed Integer Linear Programming (MILP) model.

Airport layout

We assume a taxiing system consisting of service roads (used only by ETVs at speed v^S) and taxiways (used by aircraft or ETV + aircraft combinations at speed v^X). The taxiing system is represented by a graph G , which is the union of a taxiway graph $G^X = (N^X, E^X)$ and a service road graph $G^S = (N^S, E^S)$. The edges correspond to the service roads and taxiways, and the nodes correspond to junctions, gate groups or runway entrance/exit points. The airport is assumed to have N_{cs} charging stations for the ETVs, one of which also has the function of ETV depot n_{dp} . Fig. 1 shows an example airport with the road types indicated, as well as nodes for gates, runways and charging stations. An example of the airport traffic with electric taxiing is shown; towing vehicle 5 tows an aircraft along a taxiway towards a runway. Vehicle 6 arrives at the runway from a service road to start towing another aircraft. Vehicle 1 and 4 are charging at charging stations. Vehicle 2 and 3 wait their turn for charging, since in this example the charging capacity of the stations is limited to that of one vehicle.

Aircraft and ETV routing

The routes taken by the aircraft and vehicles are calculated in advance. Distances from any node m to n are calculated using Dijkstra's shortest path algorithm, and are indicated on G^X with $d^X(m, n)$, and on G^S with $d^S(m, n)$. The schedule is created for a time period P , which spans the interval $[t^s, t^e]$. The set of $N^{F,S}$ aircraft arriving or departing at the airport within this period form the set A^S . From the flight schedule, the scheduled landing time (SLDT) of arriving flights and the scheduled off-block time (SOBT) of departing flights are collected. They are the pick-up time t_a^p of aircraft a , the moment an ETV starts towing the aircraft. The moment an ETV stops towing the aircraft is referred to as the drop-off time t_a^d , and is calculated as:

$$t_a^d = t_a^p + d^X(n_a^p, n_a^d)/v^X = t_a^p + t^X(n_a^p, n_a^d), \quad \forall a \in A^S, \quad (1)$$

with $t^X(n_a^p, n_a^d)$ the towing time for aircraft a , and n_a^p and n_a^d its pick-up and drop-off nodes, respectively. They correspond to the gate or runway

where the pick-up or drop-off takes place, which are taken from the flight schedule. The towing distance for any aircraft $a \in A^S$ is denoted with the shorthand $d_a^X = d^X(n_a^p, n_a^d)$.

All ETVs start and end the period P at the depot n_{dp} . For every towing task, an ETV v assigned to aircraft a travels to the pick-up node n_a^p , and arrives at $t_a^p - t^c$. There the ETV connects to the aircraft, which takes a time of t^c . Between t_a^p and t_a^d the ETV tows aircraft a , and upon arrival the ETV disconnects from the aircraft until $t_a^d + t^c$. Then the ETV travels towards its next towing task or a charging station. The travel time for a non-towing ETV from node m to n is given as:

$$t^S(m, n) = d^S(m, n)/v^S, \quad \forall m, n \in N^S \quad (2)$$

The fleet of ETVs is denoted as V and has size N^V . For a more detailed description of the electric towing procedure, we refer to Zoutendijk et al. [38].

Aircraft route conflicts need to be avoided. We say an aircraft has a route conflict when (a) an aircraft is using the same node or edge as another aircraft at the same time, or (b) an aircraft is violating the minimum separation time t_{sep} ; the taxiing time between it and an aircraft taxiing in front of it. Deconflicting routes is done for all aircraft in A^S at the same time, before making the ETV-to-aircraft schedule: the routes for all aircraft in A^S are calculated. Then, we iterate through the time period P in time steps of size t_{sep} . At any time step, for every aircraft $a \in A^S$, we check whether another aircraft is planned to (a) occupy the same node as aircraft a or (b) approach aircraft a on a one-directional edge in E^X . In that case aircraft a is held at its previous node until it can proceed without a conflict with any other aircraft and the separation time is respected.

It is assumed that there is no taxiing delay for the aircraft, except due to deconflicting routes. For the ETVs it is assumed that deconflicting is not required, since the service roads are assumed to provide enough opportunities of passing other vehicles, and no separation time is required.

Electricity model for electric towing vehicles (ETVs)

The state of charge (SOC) of each ETV v is tracked during the time period P . This requires a battery capacity Q , determined by the specifications of the ETV, a charging rate P^c , determined by the specifications of the ETV and the charging station used, and a discharging rate. The discharging rate can be obtained by considering the power needed to drive an ETV, and to tow an aircraft. This power can be found using the mass, velocity and rolling resistance of the vehicle and aircraft. The power consumed by an ETV during towing at speed v^X is denoted as P^X , and the power consumed during driving at speed v^S is denoted as P^S . In this work the ETVs are assumed to travel at constant speed, without accounting for acceleration and deceleration. The energy consumption of the ETV for any (part of a) route is found using the power and the time taken to traverse the route.

In addition to the characteristics of the ETV, we define the electricity capacity of the airport charging network. The electricity that is available at the airport for various electrical processes throughout the day is referred to as the *electricity capacity profile*. The processes unrelated to ETV charging require a part of the electricity capacity. Subtracting this demand from the electricity capacity profile yields the *electricity capacity profile for ETVs*. This is the airport electricity capacity that is specifically available to charge ETVs. In order to keep track of the electricity demand at different times of day we divide the time period P in $N^T = 144$ time steps t of length $\Delta = 10$ min. The start of each time step is the time associated with the time step, e.g. $T_0 = t^s$ and $T_{N^T-1} = t^e - \Delta$. The electricity capacity for ETVs at time step t is then denoted as C_t .

3. Emissions saved by electric taxiing

Several studies determine the amount of fuel or emissions spent using aircraft taxiing and other airport surface movement, e.g. [39], who find an average of 75% reduction in fuel use when towing with diesel-powered tugs compared to regular taxiing, van Baaren and Roling [19], who arrive at 82% reduction for a large airport and 65% for a small airport, and Dzikus et al. [40], who find an average fuel saving of 2.4% of total flight fuel. In this section, we derive the amount of emissions saved per kilometre of self-taxiing that is replaced by electric towing. We consider the following assumptions:

- When calculating the emissions avoided by using electric towing, we consider only the emissions avoided by consuming less jet fuel. In this work we focus on CO₂ emissions.
- We consider towing vehicles that are electric battery-powered.
- The amount of emissions per km taxiing varies with the size of the aircraft. In this section, we calculate a value based on narrow-body aircraft, which is a lower bound for the actual value considering the mix of aircraft at the airport.
- When calculating the energy spent by ETVs, we consider only the energy spent while towing aircraft, since towing aircraft takes many times more energy than driving. This can be seen by comparing towing and driving power in Section 6.

Gross taxi emissions saved

We are interested to find an estimation for the emissions saved by towing an aircraft for 1 km instead of it self-taxiing that distance. We start with finding the fuel spent while self-taxiing an aircraft.

From the work of Zhang et al. [41] we obtain that an A320 aircraft spends 88.0 kg jet fuel when taxiing a 2.5 km route at Shanghai Pudong Airport (ZSPD). In this calculation, acceleration, deceleration and idling have been included. Using these values leads to a value of 35.2 kg of jet fuel per km of taxiing for a narrow-body aircraft.

It is known that using jet fuel in an aircraft engine leads to 3.16 kg CO₂ per kg of jet fuel, see e.g. [42]. This leads to an emission saving of 111 kg CO₂ per km of taxiing.

$$C_{km}^G = C_{kg \text{ CO}_2} F_{tow}/d = 111 \text{ kg CO}_2, \quad (3)$$

where C_{km}^G is the gross amount of emissions saved per km taxiing, $C_{kg \text{ CO}_2}$ the amount of emissions per kg jet fuel, F_{tow} the average amount of jet fuel used during one towing event, and d the taxied distance during this towing event.

Net taxi emissions saved

From the flight schedule for 27-12-2021 at Schiphol [43] we obtain an average taxiing distance of 3.79 km. From the energy consumption model in Section 2, we find that the energy needed for an average tow of a narrow-body aircraft at Schiphol is 19.9 kWh. From Scarlet et al. [44] we obtain that the carbon intensity of electricity generation in Europe was 0.334 kg CO₂/kWh in 2019. This means that during the generation of the electricity needed to tow an aircraft for 1 km, 1.75 kg CO₂ is emitted. In summary, under the assumptions described above, we obtain that for each km of electric towing, 109 kg CO₂ is saved when comparing the process of electric taxiing to self-taxiing. In this paper, we will use this value to calculate emission savings obtained from distances travelled using electric towing.

$$C_{km}^N = C_{km}^G - C_{km}^E = C_{km}^G - \frac{E_{tow} E_{el}}{d_{av}} = 111 - 1.75 = 109 \text{ kg CO}_2, \quad (4)$$

where C_{km}^N is the net amount of emissions saved per km taxiing, C_{km}^E the amount of emissions spent generating electricity per km taxiing, E_{tow} the energy needed for an average narrow-body aircraft tow, d_{av} the average towing distance per aircraft movement, and E_{el} the carbon intensity of electricity generation.

Total flight emissions

In addition to estimations of the absolute amount of emissions saved using this technology, it is insightful to obtain an estimate for the effect of optimizing the emission savings of electric towing on the total flight emissions. An example of total fuel consumption of a narrow-body, medium-haul flight is given in [45]: an A320 aircraft on a flight between Los Angeles and New York uses 11.6 tons of jet fuel. If we assume two taxiing events similar to the one at Shanghai Airport, and note again that CO₂ emissions are directly proportional to fuel consumption through the factor 3.16, we obtain that using electric taxiing saves 1.5% of the total flight emissions for this flight example:

$$\frac{C_{\text{saved}}}{C_{\text{total}}} = \frac{2F_{\text{tow}}}{F_{\text{total}}} = \frac{2 \cdot 88.0}{11.6 \cdot 10^3} = 1.5\%, \quad (5)$$

with $\frac{C_{\text{saved}}}{C_{\text{total}}}$ the fraction of saved total flight emissions, and F_{total} the total fuel consumption spent on the indicated flight.

4. Mathematical formulation for vehicle-to-aircraft scheduling

In this section we formulate the mixed-integer linear program (MILP) for ETV-to-aircraft assignment, adapted from [46]. Note that a glossary with terms and notation used in this work can be found in the appendix.

First, we introduce a set of N^V artificial aircraft A^e . The aircraft $a \in A^e$ have $n_a^p = n_a^d = n_{\text{dp}}$, $d_a^X = 0$ and $t_a^d = t_a^p = t^e$. Such artificial aircraft are necessary to enforce a state of charge value for every vehicle v at the end time t^e . All artificial aircraft will always be scheduled for electric towing, at no cost. The set of all aircraft will be denoted as $A = A^S \cup A^e$ with size $N^F = N^{F,S} + N^V$. Furthermore, we introduce notation describing various quantities of energy, required in the MILP:

$$q^X(a) = P^X t^X(n_a^d, n_a^d) \quad \forall a \in A, \quad (6)$$

$$q^S(n, m) = P^S t^X(n, m) \quad \forall m, n \in N^S, \quad (7)$$

$$q^S(a, b) = q^S(n_a^d, n_b^p) \quad \forall a, b \in A, \quad (8)$$

$$q_f^S(a) = q^S(n_{\text{dp}}, n_a^p) \quad \forall a \in A, \quad (9)$$

$$q^C(a, b) = \min_{i \leq N_{\text{cs}}} \{q^S(n_a^d, n_{\text{cs},i}) + q^S(n_{\text{cs},i}, n_b^p)\} \quad \forall a, b \in A, \quad (10)$$

$$q_1^C(a) = \min_{i \leq N_{\text{cs}}} \{q^S(n_{\text{cs},i}, n_a^p)\} \quad \forall a \in A, \quad (11)$$

$$q_2^C(a) = \min_{i \leq N_{\text{cs}}} \{q^S(n_a^d, n_{\text{cs},i})\} \quad \forall a \in A, \quad (12)$$

$$t^C(a, b) = \max(t_b^p - t_a^d - t^S(n_a^d, n_b^p) - 2t^c, 0) \quad \forall a, b \in A, \quad (13)$$

with $q^X(a)$ the energy needed to tow aircraft a on G^X , $q^S(n, m)$ the energy needed by an ETV to travel from node n to m on G^S , $q^S(a, b)$ the energy needed by an ETV to travel from the dropoff point of aircraft a to the pickup point of aircraft b on G^S , $q_f^S(a)$ the energy needed by an ETV to travel from the depot n_{dp} to the pickup point of aircraft a , $q^C(a, b)$ the minimal energy needed by an ETV to travel from the dropoff point of aircraft a to the pickup point of aircraft b on G^S , via a charging station $n_{\text{cs},i}$, $q_1^C(a)$ the energy needed by an ETV to travel from the closest charging station to the pickup point of aircraft a , $q_2^C(a)$ the energy needed by an ETV to travel from the dropoff point of aircraft a to the closest charging station, and $t^C(a, b)$ the time between towing consecutive aircraft a and b that is freely available to the ETV towing them.

Using $t^C(a, b)$ and the set of aircraft A , we define:

$$A_a^{\text{out}} = \{b \in A : t^C(a, b) > 0\} \quad \forall a \in A, \quad (14)$$

$$A_a^{\text{in}} = \{b \in A : t^C(b, a) > 0\} \quad \forall a \in A, \quad (15)$$

$$A_a^{\text{PC}} = \{b \in A_{\text{out}}(a) : q^C(a, b) - q^S(a, b) < P^c(t^C(a, b) - t_{\text{min}}^C)\} \quad \forall a \in A. \quad (16)$$

Here A_a^{out} is the set of aircraft that can be towed by an ETV after it tows aircraft a , A_a^{in} is the set of aircraft that can be towed by an ETV before it tows aircraft a , and A_a^{PC} is the set of aircraft that can be towed by an ETV after it tows aircraft a and for which there is at least t_{min}^C time in between for effective charging, which is charging that occurs after the energy loss due to the rerouting to the charging station has been replenished. The time t_{min}^C is called the *minimum charging time*. Note that $A_a^{\text{PC}} \subseteq A_a^{\text{out}}$.

For brevity, define v_a as the vehicle v that tows aircraft a . Furthermore, we define $M \in \mathbb{R}$ as a large number. We consider the following decision variables:

$$x_{ab} = \begin{cases} 1 & \text{if } a, b \in A \text{ are towed consecutively} \\ 0 & \text{else} \end{cases} \quad (17)$$

$$x_a^f = \begin{cases} 1 & \text{if } a \in A \text{ is the first aircraft an ETV tows} \\ 0 & \text{else} \end{cases} \quad (18)$$

$$x_a^l = \begin{cases} 1 & \text{if } a \in A \text{ is the last aircraft an ETV tows} \\ 0 & \text{else} \end{cases} \quad (19)$$

$$q_a \in [q^X(a), Q] \quad \text{ETV state of charge at the start of towing } a \in A \quad (20)$$

$$c_a = \begin{cases} 1 & \text{if after towing aircraft } a, \text{ the ETV travels to a} \\ & \text{charging station and is charged} \\ 0 & \text{else} \end{cases} \quad (21)$$

$$c_a^t \in [0, Q/P^c] \quad \text{charging time of ETV } v_a \quad (22)$$

$$c_a^s \in T \quad \text{start time of charging of ETV } v_a \quad (23)$$

$$\alpha_{at} = \begin{cases} 1 & \text{if charging of ETV } v_a \text{ starts earlier than timestep } t \\ 0 & \text{else} \end{cases} \quad (24)$$

$$\beta_{at} = \begin{cases} 1 & \text{if charging of ETV } v_a \text{ finishes later than timestep } t \\ 0 & \text{else} \end{cases} \quad (25)$$

$$\gamma_{at} = \begin{cases} 1 & \text{if ETV } v_a \text{ is charged during timestep } t \\ 0 & \text{else} \end{cases} \quad (26)$$

$$y_a = \begin{cases} 1 & \text{if } a \in A \text{ is towed by an ETV} \\ 0 & \text{if } a \in A \text{ is taxiing by itself} \end{cases} \quad (27)$$

The objective function and constraints are given by:

$$\max_{x, q, y, c} \sum_{a \in A} d_a^X y_a, \quad (28)$$

$$\text{s.t. } x_a^f + \sum_{b \in A_a^{\text{in}}} x_{ba} = y_a \quad \forall a \in A, \quad (29)$$

$$\sum_{b \notin A_a^{\text{in}}} x_{ba} = 0 \quad \forall a \in A, \quad (30)$$

$$x_a^l + \sum_{b \in A_a^{\text{out}}} x_{ab} = y_a \quad \forall a \in A, \quad (31)$$

$$\sum_{b \notin A_a^{\text{out}}} x_{ab} = 0 \quad \forall a \in A, \quad (32)$$

$$q_a \leq x_a^f(Q - q_f^S(a)) + Q(1 - x_a^f) \quad \forall a \in A, \quad (33)$$

$$q_a \geq x_a^f(Q - q_f^S(a)) - Q(1 - x_a^f) \quad \forall a \in A, \quad (34)$$

$$q_b \leq q_a - x_{ab}(q^X(a) + q^S(a, b)) + Q(1 - x_{ab}) \quad \forall a \in A, b \in A_a^{\text{out}} \setminus A_a^{\text{PC}}, \quad (35)$$

$$q_b \geq q_a - x_{ab}(q^X(a) + q^S(a, b)) - Q(1 - x_{ab}) \quad \forall a \in A, b \in A_a^{\text{out}} \setminus A_a^{\text{PC}}, \quad (36)$$

$$q_b \leq q_a - x_{ab}(q^X(a) + q^C(a, b)) + (1 - c_a)(q^C(a, b) - q^S(a, b)) + P^c c_a^t + Q(1 - x_{ab}) \quad \forall a \in A, b \in A_a^{\text{PC}}, \quad (37)$$

$$q_b \geq q_a - x_{ab}(q^X(a) + q^C(a, b)) + (1 - c_a)(q^C(a, b) - q^S(a, b)) + P^c c_a^t - Q(1 - x_{ab}) \quad \forall a \in A, b \in A_a^{\text{PC}}, \quad (38)$$

$$N^V \geq \sum_{a \in A} x_a^f, \quad (39)$$

$$y_a = 1 \quad \forall a \in A^e, \quad (40)$$

$$q_a \geq q^e \quad \forall a \in A^e, \quad (41)$$

$$c_a^s \geq t_a^d + t^c + q_2^C(a)/P^S - M(1 - c_a) \quad \forall a \in A, \quad (42)$$

$$c_a^s + c_a^t \leq t_b^p - t^c - q_1^C(b)/P^S + M(1 - x_{ab}) + M(1 - c_a) \quad \forall a \in A, b \in A_a^{\text{out}}, \quad (43)$$

$$c_a^t \geq t_{\min}^C c_a \quad \forall a \in A, \quad (44)$$

$$c_a^t \leq \sum_{b \in A_a^{\text{PC}}} x_{ab} t^C(a, b) \quad \forall a \in A, b \in A_a^{\text{PC}}, \quad (45)$$

$$c_a \geq M^{-1} c_a^t \quad \forall a \in A, \quad (46)$$

$$c_a^s \leq T_t + \Delta + M(1 - \alpha_{at}) \quad \forall a \in A, t \in P, \quad (47)$$

$$c_a^s \geq T_t + \Delta - M\alpha_{at} \quad \forall a \in A, t \in P, \quad (48)$$

$$c_a^s + c_a^t + M(1 - \beta_{at}) \geq T_t \quad \forall a \in A, t \in P, \quad (49)$$

$$c_a^s + c_a^t - M\beta_{at} \leq T_t \quad \forall a \in A, t \in P, \quad (50)$$

$$\gamma_{at} \geq \alpha_{at} + \beta_{at} - 1 \quad \forall a \in A, t \in P, \quad (51)$$

$$\gamma_{at} \leq \alpha_{at} \quad \forall a \in A, t \in P, \quad (52)$$

$$\gamma_{at} \leq \beta_{at} \quad \forall a \in A, t \in P, \quad (53)$$

$$P^c \sum_{a \in A} \gamma_{at} \leq C_t \quad \forall t \in P. \quad (54)$$

The objective (28) is to maximize the total towing distance by the ETV fleet. Constraints (29) and (31) ensure that every aircraft a that is towed by an ETV, is either the first (last) to be towed by an ETV, or has another aircraft b preceding (following) it. Constraints (30) and (32) ensure that any aircraft b cannot precede (follow) aircraft a , if $b \notin A_a^{\text{in}} (A_a^{\text{out}})$. Constraints (33) and (34) set the state of charge of all vehicles at the start of their first towing task. Constraints (35)–(38) set the new state of charge of a vehicle after towing aircraft a . Constraints (35)–(36) concern towing an aircraft without charging afterwards and Constraints (37)–(38) concern towing and charging. Constraint (39) enforces the fleet size of N^V . Constraints (40)–(41) define the artificial flights in A^e . Constraints (42)–(43) set the earliest time for a charging period to start and the latest time for it to end. Constraints (44)–(45) set the bounds for the charging time, based on the minimum charging time t_{\min}^C and the maximum possible charging time for the aircraft a and b . Constraint (46) sets the charging indicator c_a to 1 if the charging time c_a^t is strictly positive. Finally, Constraints (47)–(53) keep track of the time steps during which an ETV is being charged, so that this can be limited to the electricity capacity for ETVs at time step t with Constraint (54).

The MILP is solved using Gurobi. Recall that the goal is to create an ETV-to-aircraft schedule for a full day. The number of constraints in the model is bounded by $9N^F + 6N^{F^2} + 2N^V + 7N^F N^T + N^T$. The MILP model is expected to have a large runtime. An effective way to

reduce the number of constraints is to adapt Eqs. (14)–(15) in such a way that an aircraft b that is scheduled more than e.g. a few hours later than aircraft a will not appear in A_a^{out} . Nevertheless, the number of constraints grows roughly quadratically with N^F . Solving the MILP model is feasible for time periods of a few hours, but becomes intractable for periods P longer than 8 h. Another approach is necessary, and such an approach will be introduced in the following section.

5. An ALNS approach to electricity capacitated ETV scheduling

The MILP formulation introduced in Section 4 is not able to provide a solution for problem instances of a full day. To find such solutions, we present here a heuristics-based approach to the ETV-to-aircraft assignment problem. The approach is based on the framework of Adaptive Large Neighbourhood Search (ALNS), originally developed by Ropke and Pisinger [47].

ALNS algorithms work by removing a relatively large part of a given solution, and then building a new solution with new values. Which part of the solution is removed or inserted is governed by several removal and insertion heuristics, respectively. It is desirable to explore new solutions without getting stuck in local minima. The local search framework ensures that not all candidate solutions obtained are accepted.

The ALNS metaheuristic has been chosen because of the possibility to develop insertion and removal heuristics tailored to the problem. For the ETV scheduling problem, it is important to keep precise track of the locations and state of charge of every vehicle. Furthermore, the scheduled tasks have a fixed time, and cannot be reordered, nor can the problem be split in parts without compromising the goal of investigating the effects of the electricity capacity on the effectivity of operations throughout the whole day. This reduces the options for decomposition or relaxation of the problem, on which many other heuristics are based.

5.1. Adapting ALNS for ETV to aircraft scheduling

The ALNS algorithm cannot be used directly for the ETV-to-aircraft scheduling problem. Some alterations and definitions are necessary, and are discussed in this section.

First, we define a solution s , representing a towing schedule, as a vector of the decision values introduced in Section 2. The objective value associated with s is denoted as $f(s)$, and calculated as in Eq. (28). Algorithm 1 shows the procedure followed in the ALNS algorithm, adapted from Ropke and Pisinger [47] and Pisinger and Ropke [48]. In this section, the steps in the algorithm are clarified.

Feasible steps

The removal and insertion heuristics select certain aircraft from a given solution s to remove or insert. The aircraft are then removed or inserted sequentially, if the resulting solution is feasible. Not all aircraft can be readily removed from the solution or added to it, without breaking some of the Constraints (29)–(54), most pertinently Constraints (41), (44), and (54). This means that when applying a heuristic, it should be known for every aircraft whether it may or may not be removed or inserted from the current schedule. We view the situation after removing or inserting any single aircraft as a new *solution step*. These steps are not stored during the ALNS algorithm. While applying the removal and insertion requests from the heuristic, the algorithm first calculates whether it is allowed for an aircraft to be inserted or removed from the current solution step, and if it is not, the aircraft is skipped. If it is allowed, the insertion or removal is executed, and the relevant decision variables are changed. At any point during the algorithm, the set of aircraft that are allowed to be removed is denoted as A^{rem} , and the set of aircraft that are allowed to be inserted into the schedule of vehicle v is denoted as A_v^{ins} .

Algorithm 1 Adaptive Large Neighborhood Search for ETV-to-aircraft assignment

Require: s^l initial solution (Section (5.1)), N^-, N^+ number of removal and insertion heuristics, $\sigma_1, \sigma_2, \sigma_3$ score values, N^{seg} segment length.

- 1: $s^b = s^l = s^i, \quad s^{\text{all}} = \{s^l\}$.
- 2: $\bar{\pi}^- = \pi^- = [1/N^-, \dots, 1/N^-], \quad \bar{\pi}^+ = \pi^+ = [1/N^+, \dots, 1/N^+]$.
- 3: **for** $k = 1, 2, \dots, N_{\text{it}}^{\text{do}}$
- 4: Select removal and insertion heuristic h_i^+ and h_j^- using π^+ and π^- (Section (5.2.2)-(5.2.3)).
- 5: $s^c = h_i^+(h_j^-(s^l))$
- 6: **if** $f(s^c) > f(s^b)$ **then**
- 7: $s^b = s^l = s^c, \quad s^{\text{all}} = s^{\text{all}} \cup s^l$.
- 8: $\bar{\pi}_i^+ += \sigma_1, \quad \bar{\pi}_j^- += \sigma_1$
- 9: **else if** s^c not in s^{all} and $f(s^c) > f(s^l)$ **then**
- 10: $s^l = s^c, \quad s^{\text{all}} = s^{\text{all}} \cup s^l$.
- 11: $\bar{\pi}_i^+ += \sigma_2, \quad \bar{\pi}_j^- += \sigma_2$
- 12: **else if** s^c not in s^{all} and s^c is accepted (Section (5.3)) **then**
- 13: $s^l = s^c, \quad s^{\text{all}} = s^{\text{all}} \cup s^l$.
- 14: $\bar{\pi}_i^+ += \sigma_3, \quad \bar{\pi}_j^- += \sigma_3$
- 15: **end if**
- 16: **if** $\text{mod}(k, N^{\text{seg}}) = 0$ **then**
- 17: Calculate π^- and π^+ (Section 5.2.1)
- 18: **end if**
- 19: **end for**

When an aircraft a is added to the towing schedule of an ETV, the total energy required by that ETV will increase. To make sure that Constraint (41) is respected, the vehicle should recharge longer. An existing charging period is selected and lengthened where allowed (w.r.t Constraint (54)). If there is no charging period that can be lengthened, the addition of a is not allowed. Similarly, when removing an aircraft a , a charging period should be shortened. In that case it is important that Constraint (44) is still respected for each charging period.

Moving charging periods

Note that the removal and insertion heuristics can only lengthen and shorten existing charging periods. The heuristics cannot be used to move a charge period within the time period, or split or merge charging periods. For this reason, the model might not be able to reach all feasible (and possibly better) solutions. To make this possible, the model includes a procedure to change charging periods within schedules.

For every pair of aircraft that are towed consecutively, we name the period of time in between the *task gap*. A task gap can contain a charging period. When (a part of) a charging period is moved from one task gap to another, the former is named the *donator* and the latter the *receiver*. For every existing charging period, we calculate the amount of charge that may be moved to a different task gap. This amount is named the *available charge*. Here we take into account the minimum charging time t_{\min}^C of both the receiver and donator task gaps, as well as the bounds for the state of charge q_a of the vehicle at its arrival at any of the aircraft it will tow. From all existing charging periods with positive available charge, one is selected randomly. The available charge is moved from the donator to the receiver by changing the associated decision variables. If none of the charging periods have positive available charge, no changes are made. In every ALNS iteration k , this procedure is performed $\lceil 0.2N^V \rceil$ times between using the removal and insertion heuristic and then once more after using the insertion heuristic. It was found that increasing the occurrence of the moving charge procedure did not improve the ALNS solution finding process.

Another way of changing the charging periods would be to introduce charging station removal and insertion heuristics, in addition to

the current aircraft removal and insertion heuristics. Such an approach was taken by Keskin and Çatay [15]. We opted for the above method, because it allows the moving of charging periods during the removal and insertion of aircraft, where more options for charge movement are possible, rather than only in between applying heuristics.

Initial solution

Before the algorithm starts using the removal and insertion heuristics, it needs an initial solution s^l . The initial solution should be a feasible solution to Problem (28)–(54), and it should be possible to move to other solutions by adding and removing aircraft and changing charging periods. Note that e.g. the solution with only the aircraft in A^e and no charging is feasible, but other solutions are unreachable from this solution due to Constraint (44).

Given the capacity profile for ETVs, period P and flight schedule, a valid initial solution can readily be constructed:

- For every vehicle, assign several aircraft that need to be towed near the start of P , and together need more than the minimum charging time t_{\min}^C to be replenished.
- For every vehicle, calculate the needed charging time to replenish the battery. Set this charging in such a place that Constraint (54) is respected: start by putting charging periods for each vehicle near the end of P , moving backwards in time when required by this constraint.

The initial solution thus constructed can serve as input for the removal and insertion heuristics, which will be introduced next.

5.2. Local search heuristics

The choice of local search heuristics for removal and insertion is an essential part of the ALNS algorithm. Selecting a diverse set of heuristics contributes to the ability of the algorithm to explore the solution space and to escape local minima [48]. The heuristics in the set are being used throughout the run of the algorithm, and are selected with weighted random selection.

5.2.1. Heuristic weights

The weight updates are performed as described by Pisinger and Ropke [48]. The total number of ALNS iterations is divided into equally sized segments. Two sets of scores exist: the *segment score* $\bar{\pi}_{i,j}^-$ and the *overall score* $\bar{\pi}_{i,j}^-$ for removal heuristic i and iteration segment j . Similarly, we have scores $\bar{\pi}_{i,j}^+$ and $\pi_{i,j}^+$ for the insertion heuristics. The segment score has an initial value of 0 at the beginning of every segment. During the segment, the segment score is increased with scores that depend on the quality of the candidate solution s^c :

- The candidate solution is a new best solution: increase segment score by σ_1
- The candidate solution has a larger objective function than the latest solution s^l : increase segment score by σ_2
- The candidate solution has a smaller objective function than the latest solution but is accepted by the local search framework: increase segment score by σ_3
- The candidate solution is not accepted by the local search framework: the segment scores remain the same.

Here $\sigma_1 \geq \sigma_2 \geq \sigma_3$. At the end of segment j the overall scores are calculated with:

$$\pi_{i,j+1}^- = \rho \frac{\bar{\pi}_{i,j}^-}{a_{i,j}^-} + (1 - \rho)\pi_{i,j}^-, \quad (55)$$

with ρ the reaction factor and $a_{i,j}^-$ the amount of times removal heuristic i has been selected in segment j . The overall insertion scores are calculated analogously. Finally, the overall scores π^- and π^+ are normalized, and the result forms the updated heuristic weights.

5.2.2. Removal heuristics

In previous research regarding vehicle routing problems and scheduling problems, many removal and insertion heuristics have been developed. Some heuristics used in this work are taken or adapted from existing literature. In a typical application of ALNS for routing and scheduling problems, tasks can be inserted at other times and in different orders compared to previous solution. By contrast, in our application, the time of a towing tasks always remains the same. In addition, removal and insertion is complicated by restrictions regarding the state of charge and allowed charging moments of vehicles. This means that, in contrast to works such as Frey et al. [17], we opted to disallow moving through infeasible regions of the solution space. Repairing an infeasible solution is expected to be difficult to automate and to be costly in computation time, given the many constraints in this problem.

We use six removal heuristics:

1. *Random removal* (from [47]). Select N^{rem} aircraft randomly from A^{rem} and remove these from the schedule.
2. *Vehicle removal*. For every ETV, select one aircraft that is currently in its towing schedule and in A^{rem} , and remove that aircraft from the schedule.
3. *Cluster removal* (from [48]). Consider the ETV that tows the fewest aircraft during the schedule from all ETV in the fleet. Remove as many aircraft as possible from the schedule of that vehicle. This will leave a few aircraft and one charging period with charging time near t_{\min}^C . The idea of this heuristic is that if the schedule for an ETV is stuck in a suboptimal position, one can take out everything for that ETV and start over.
4. *Time-oriented removal* (from [48]). Select randomly a time period of one hour in P . Remove as many aircraft as possible for which the towing period lies within this interval. This heuristic allows for a reorganization of the schedule around a time period, which can help resolve possible charging capacity conflicts in that period.
5. *Worst removal* (after [47]). For every aircraft in the schedule and in A^{rem} : calculate the amount of time in the task gap between the aircraft and its successor, and between its predecessor and itself (where applicable). Note that this is the time $t^C(a, b)$ defined in Eq. (13). Then select the aircraft with the largest average task gap length for removal. Repeat until N^{rem} aircraft have been removed. This heuristic is based on the notion that aircraft with more task gap length before and after their scheduled towing time can easier be assigned a more efficient place in the schedule.
6. *Time-based worst removal*. For every aircraft in the schedule and in A^{rem} , calculate the travelling energy q^{travel} saved by removing the aircraft from the schedule. For example, when towing an aircraft b after towing aircraft a and before towing aircraft c :

$$q_b^{\text{travel}} = q^S(a, b) + q^S(b, c) - q^S(a, c). \quad (56)$$

Then select the aircraft with the largest saved travelling energy for removal. Repeat until N^{rem} aircraft have been removed. This heuristic aims to optimize the route of an ETV and avoid large detours.

5.2.3. Insertion heuristics

We use four insertion heuristics. For all insertion heuristics, the procedure described below is repeated until no more aircraft can be inserted. All selected insertion heuristics are of the parallel category; they build on the routes of the entire problem at the same time, not one ETV at once.

1. *Random insertion* (from [47]). Consider all aircraft and vehicle combinations in A_v^{ins} . Select one randomly and insert the aircraft into the schedule of that vehicle.

2. *Greedy towing distance insertion*. Consider the vehicle v^g that has the most total task gap length in its schedule. Let S_v^{pair} be the set of aircraft pairs towed consecutively by vehicle v . Then v^g is selected as in Eq. (58).

$$S_v^{\text{pair}} = \{\{a, b\} \in [A \times A] : a \text{ is towed by } v \wedge x_{ab} = 1\} \quad \forall v \in V \quad (57)$$

$$v^g = \max_{v \in V} \sum_{\{a, b\} \in S_v^{\text{pair}}} t^C(a, b) \quad (58)$$

Consider all aircraft in $A_{v^g}^{\text{ins}}$. Insert the aircraft with the largest towing distance.

3. *Greedy tight insertion*. Iterate through all vehicles in the fleet. Given vehicle v , consider all aircraft in A_v^{ins} . Insert the aircraft for which the task gap length $t^C(a, b)$ between its predecessor and itself or between itself and its successor is minimized. The goal is to put aircraft as close together as possible in the towing schedule of an ETV, so that more aircraft might be added to the schedule. This heuristic is the opposite of removal heuristic 5.
4. *Time-based best insertion*. Iterate through all vehicles in the fleet. Given vehicle v , consider all aircraft in A_v^{ins} , and calculate the travelling energy needed to insert the aircraft into the schedule, as for the time-based worst removal heuristic (nr. 6). Then select the aircraft with the smallest needed travelling energy for insertion. Like its counterpart in the removal heuristics, this heuristic aims to optimize the route of an ETV by inserting aircraft that lead to the smallest detours.

Note that for all removal and insertion heuristics, removing/inserting an aircraft will only be performed if it does not result in an infeasible solution (see also Section 5.1). Furthermore, aircraft in A^e are never considered for removal/insertion, as they are always in the schedule.

5.3. Local search framework

The local search framework is the mechanism that decides whether a candidate solution s^c is accepted or rejected. After applying a removal and insertion heuristic the candidate solution is checked using Simulated Annealing and Tabu Search.

Simulated Annealing [49] is a method that aims to guide the local search towards the global optimum. At the start of the search, it allows for more exploration, while near the end of the search, exploration is restricted, and improvement of the objective value is increasingly required for a solution to be accepted.

During the search, Simulated Annealing makes use of the *temperature* parameter T . At the beginning, the temperature has value $T = T^{\text{st}}$. At every iteration of the ALNS algorithm, the temperature is decreased as $T := Tc$, with $0 < c < 1$. To set the value of T^{st} , the method uses the *start temperature control parameter* w . At the start of the algorithm, a candidate solution s^c may be $w\%$ worse than the latest solution s^l to be accepted with probability 0.5. As the algorithm progresses, the acceptance probability for a given T and w decreases, following Eq. (59):

$$p^{\text{accept}} = e^{-(f(s^l) - f(s^c)) / f(s^l) / T} \quad (59)$$

Setting c and w correctly for a given problem instance requires trial and error. Model parameters that have a large influence on the optimal values for c and w are the length of the time period P , the fleet size N^V and the number of flights N^F .

In addition to the check performed by Simulated Annealing, we make sure that the candidate solution s^c has not been accepted before, i.e. we incorporate Tabu Search [50].

Table 1
Parameters used in the scheduling models and their standard values.

Symbol	Name	Value	Unit	Source
ETV properties				
P^c	Charging rate	100	kW	van Oosterom et al. [52]
P^X	Towing power	222	kW	Zoutendijk et al. [46]
P^S	Driving power	20.5	kW	Zoutendijk et al. [46]
Q	Battery capacity	400	kWh	van Oosterom et al. [52]
v^s	Speed on service roads	30	km/h	Schiphol [53] and Munich International Airport [54]
v^x	Speed on taxiways	42	km/h	Smart Airport Systems [3]
t^c	Connecting/Disconnecting time	3.0	min	Schiphol [55]
Airport infrastructure				
t_{sep}	Separation time	20	s	Zoutendijk et al. [46]
t_{min}^c	Minimum charging time	30	min	
Δ	Time step	10	min	
N_{cs}	Number of charging stations	3	–	
ALNS algorithm				
N^{it}	Number of ALNS iterations	1000	–	
N^{seg}	Nr of iterations in ALNS segment	10	–	
N^{rem}	Nr of aircraft removed in heuristic	N^V	–	
Simulated Annealing				
σ_1	Global solution reward	2	–	
σ_2	Previous solution reward	0.6	–	
σ_3	Accepted solution reward	0.2	–	
ρ	Reaction factor	0.25	–	
w	Start temperature control parameter	1.05	–	
c	Cooling rate	0.997	–	

Table 2
Parameter values of problem instances ran with the models. Times indicated are on 27th (to 28th) of December 2021.

Instance	P	N^V	N^F	N^{it}	c	w	t_{min}^c
1	08:00–14:00	4	49	2500	1.10	0.9993	20
2	18:00–04:00	4	57	4000	1.25	0.9985	30
3	04:00–04:00	2	80	4000	1.25	0.9980	30
4	04:00–04:00	4	138	4500	1.25	0.9985	30
5	04:00–04:00	6	193	3500	1.25	0.9985	30

6. Results

In this section results are presented that are obtained by applying the models introduced in Sections 4 and 5 to historical flight schedules at Amsterdam Airport Schiphol. The schedules are obtained from the Schiphol Flight API within the Schiphol Developer Center [43]. For each flight, the schedules contain the gate number and scheduled and actual arrival/departure times. The runway for each flight is found from runway use data [51]. A general overview of parameters contained in the models is provided in Table 1. The values indicated in the table are the standard values for our model, and are used unless otherwise indicated.

6.1. Model comparison with small scale problem instances

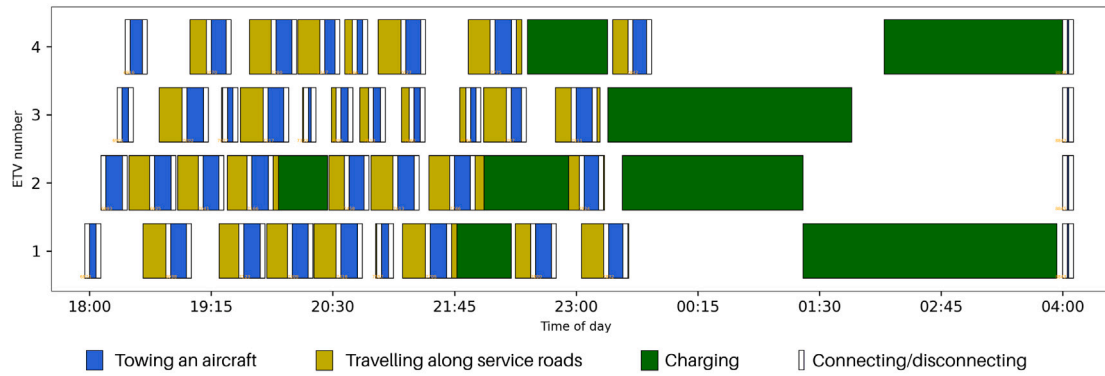
In order to illustrate the performance of the MILP and ALNS models, several problem instances have been defined, summarized in Table 2. All instances refer to the flight schedule of 27-12-2021 (or up until 04:00 on the day after) at Amsterdam Airport Schiphol. The capacity profile for each instance in Table 2 is given by: 100% capacity during 04:00–06:00 and 23:00–04:00, 200 kW capacity elsewhere. Parameters not appearing in this table have the values as indicated in Table 1. The values of N^{it} , c and w have been manually tuned for each instance to obtain the best performance.

Fig. 2 shows a side-by-side comparison of example results for the ALNS and MILP models, for a run of instance 2. These schedules show for each ETV when it is towing an aircraft, travelling along service roads, connecting/disconnecting to/from an aircraft, or charging at a charging station. For this instance, 40 (out of 57 possible) aircraft are

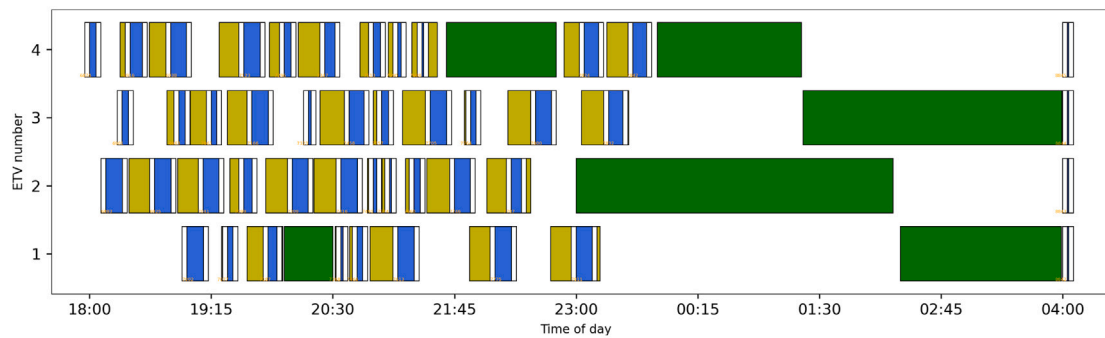
towed by 4 ETVs in the optimal solution. In the solution created by ALNS, more aircraft are towed, but the total towing distance, and therefore the emission savings, are lower. By optimizing for total towing distance, the models are incentivized to schedule towing tasks with longer towing distance, rather than as many short tasks as possible.

The ALNS solution shown is the best solution found after 4000 iterations. The selection probability at a certain iteration for each removal or insertion heuristic is a measure for its effectiveness in improving the solution during the previous iterations. Fig. 3 shows the selection probabilities of all removal and insertion heuristics, listed in Sections 5.2.2–5.2.3, for twenty runs of problem instance 2. Observing the average selection probabilities provides insight in the usefulness of each heuristic. For example, random removal and insertion (nrs. 1) perform well, despite their simple nature. Greedy insertion (nr. 2) also performs well, especially for schedules with larger fleet size. This likely happens because it pushes to insert the tasks with the larger towing distance. On the other hand, time-based removal (nr. 6) and time-based insertion (nr. 4) perform worst. On many occasions, the selection probability of time-based removal converges towards zero. The average towing distance of towing tasks added by time-based insertion is the smallest of all insertion heuristics. Similarly, the average towing distance of towing tasks removed by time-based removal is the largest of all removal heuristics. Rather than achieving their goal of minimizing detours in the ETV route, the heuristics seem to avoid longer towing tasks. This is because a longer towing task is more likely to constitute a large detour for an ETV than a shorter towing task.

We now examine the performance of the MILP and ALNS models for all instances introduced in Table 2. Note that the number of flights N^F indicated in Table 2 is not the total number of flights passing through the airport during the time period P . The number of flights eligible for towing has been reduced to accommodate the MILP model: with a smaller N^F value, the solution time is greatly reduced, since fewer decision variables and constraints are generated (see Section 4). In addition, if the amount of scheduled aircraft in an optimal solution is close to the number of total available flights, the scheduling problem becomes easier than with a larger total of available flights, due to combinatorics. These problem instances allow us to compare both models equally. Nevertheless, the MILP model does not find the optimal solution for instance 3–5. For comparison with the ALNS model, the best incumbent solution and best bound are used.



(a) An optimal schedule with 40 aircraft generated by the MILP model. Total towing distance 200.2 km, CO₂ emissions saved 21.9 ton, and total charging energy 1.16 MWh.



(b) A schedule with 45 aircraft generated using the ALNS algorithm for 4000 steps. Total towing distance 191.2 km, CO₂ emissions saved 20.9 ton, and total charging energy 1.07 MWh.

Fig. 2. ETV-to-aircraft schedules generated using the MILP model and ALNS algorithm, for instance 2 in Table 2. The ALNS algorithm attains a 4.5% gap compared to the MILP solution for this run.

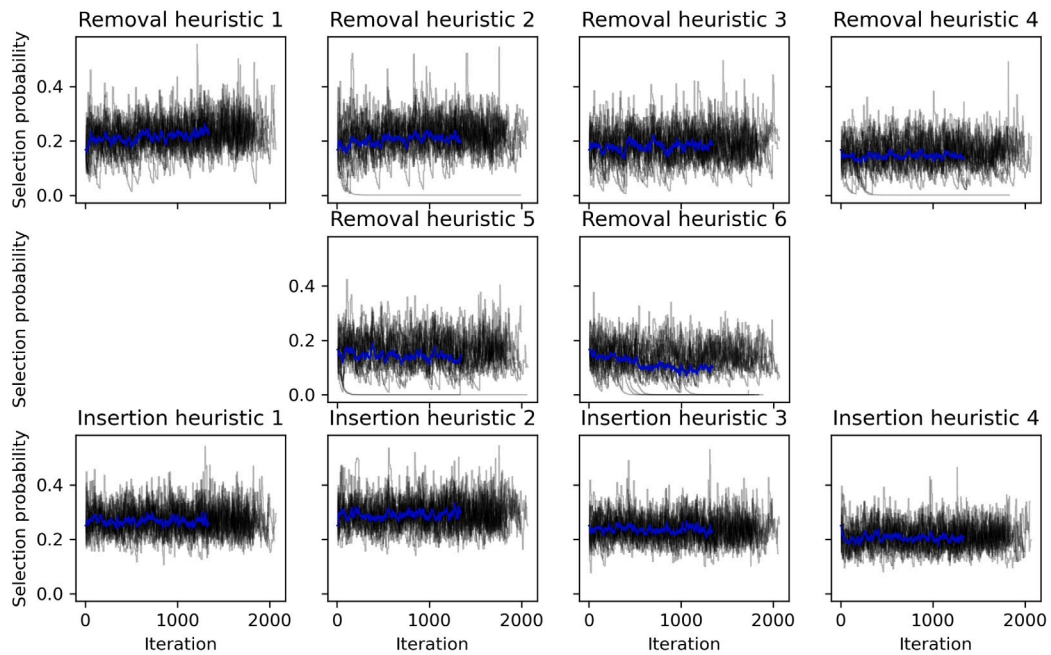


Fig. 3. The evolution of selection probabilities for all heuristics, for 20 runs with 2500 steps of the scheduling problem for 18:00–04:00 on 27-12-2021. The average is indicated by the blue line.

Table 3

Total towed distance values for solutions obtained by the MILP and ALNS models, when applied to the problem instances introduced in Table 2.

Instance Unit	MILP				ALNS			
	Opt. sol. [km]	Best sol. [km]	Best bound [km]	Runtime [min]	Best sol. [km]	Mean best sol. [km]	Gap w.r.t MILP [%]	Runtime [min]
1	141.3	–	–	1.2	129.8	123.0	8.1	1.5
2	200.2	–	–	0.1	198.8	188.3	0.7	2.6
3	–	265.0	275.2	190	247.8	243.7	6.5	7.5
4	–	508.2	527.0	188	496.8	479.2	2.2	17
5	–	712.7	719.1	241	688.0	674.8	3.5	25

Table 3 shows the objective values (total towing distance of the schedule) obtained with the MILP and ALNS models. For the MILP model, the optimal solution, best incumbent solution and best bound are indicated where applicable. The runtime for the instances without an optimal solution indicates the time the optimization process was continued for, not the time at which the best incumbent solution was found. For the ALNS model, 20 runs were performed for each problem instance. The best solution, the mean best solution (average of the best solutions of all runs) and the gap of the best ALNS solution with respect to the MILP solution (optimal or best incumbent) are given.

In addition, Fig. 4 shows graphs of convergence for the 20 runs with the ALNS model for all five instances. The average and the best run are highlighted, as well as the best result for every run. The convergence is illustrated as a gap value relative to the MILP solution (either the optimal or best incumbent). For several of the instances in the figure it seems using more iterations than shown would improve the solution further. However, this is not the case, since in fact many rejected solutions are produced between and after the shown accepted solutions, which are not included in the figure.

Table 3 and Fig. 4 show that when the period of interest P and number of flights N^F are made small enough, the MILP model finds the optimal solution fast, and is superior to the ALNS model. However, when the period of interest P comprises a full day, and the ETV fleet size N^V starts to (slightly) increase, the MILP model is unable to find the optimal solution within several hours. The best solution found through the ALNS model is close to the best incumbent solution of the MILP model. These results show that for a time frame of more than a few hours, the ALNS provides results of quality close to that of the MILP model, in a much shorter time. Note that creating a schedule with the ALNS model for any of the instances 1–5 with all aircraft that pass through the airport during their respective time period P (rather than only the selection now used) will not increase the runtime.

6.2. The impact of the electricity capacity at the airport on the ETV towing schedules

The variation of electricity capacity throughout a day of operation directly influences the ETVs' ability to recharge. In a successful ETV schedule the ETVs charge in such a way that they can perform towing tasks in as much of the time period P as possible, without running out of charge during a time when little or no charging is allowed. In other words, the ETV utilization is high. We aim to investigate the influence of the electricity capacity profile for ETVs on the schedules generated by the model.

The ETV capacity profiles are given by:

Capacity profile A: night capacity. 0% capacity during 04:00–23:00 and 100% capacity during 23:00–04:00.

Capacity profile B: overall low capacity. 40% capacity during 04:00–04:00.

Capacity profile C: no capacity during rush hour. 0% capacity during 07:00–10:00 and 16:00–19:00, 40% capacity during 10:00–16:00 and 19:00–23:00 and 100% capacity during 04:00–07:00 and 23:00–04:00.

Capacity profile D: low capacity during day. 0% capacity during 06:00–23:00 and 100% capacity during 04:00–06:00 and 23:00–04:00.

Capacity profile E: full capacity. 100% capacity during 04:00–04:00.

The profiles represent possible charging capacity situations at the airport. Note that larger charging capacity for ETV charging implies smaller charging capacity for the other processes at the airport. For example, in profile C, no capacity during rush hour implies that all capacity has been taken by other processes.

Using the ALNS model, ETV schedules have been created for each of these capacity profiles, and for several fleet sizes. In all cases, the time period P is given by a full day (between 04:00 and 04:00), in which 955 aircraft movements are planned. Fig. 5 provides a visualization of the five capacity profiles considered, for a fleet size of 10 ETVs. In addition, the electricity demand from this fleet for a scheduling solution obtained with ALNS is shown. Note that $P^c = 100$ kW, so that every 100 kW on the y -axis translates to one charging ETV at the time given on the x -axis.

In addition, Fig. 6(a) shows an overview of objective values obtained when creating ETV schedules for fleet sizes that are representative of an airport aiming to fully implement electric taxiing. For each combination of the capacity profiles A-E and fleet size value in $\{5, 10, 20, 30\}$, a boxplot is shown, which summarizes the objective values of five runs. Average runtimes for 1000 iterations of the ALNS algorithm are given by 45.1, 64.3, 125 and 199 min for fleet sizes 5, 10, 20 and 30 ETVs, respectively.

By examining Figs. 5 and 6(a), as well as the schedules generated by all runs that have been summarized in Fig. 6(a), we draw conclusions regarding the ETV electricity capacity profiles.

- We see that for every fleet size considered, only allowing night charging leads to an average decrease in total towed distance of 46% compared to the best performing profile, profile E. This shows that an ETV would need almost twice the current battery capacity to keep towing aircraft for the full day.
- For the second charging profile, we see that the limited capacity of 40% is used to the fullest from roughly 10:00 until the end at 04:00. For several ETVs the utilization time is reduced, because the ETV runs out of charge and cannot charge earlier due to the decreased capacity. The average decrease in objective value is 13%.
- The third charging profile simulates a situation where little or no electricity capacity can be reserved for charging ETVs during busy periods. For example, between 16:00–19:00 the aircraft in the schedule are atypical: for small fleet size (5 or 10), aircraft with very short towing distance are scheduled during this time. For the larger fleet sizes, the ETV utilization is low during this period, i.e. the schedule is more empty. This is because there are not enough tasks with small towing distance for all ETVs.
- Charging profile D is similar to profile B. The main difference is that night charging (23:00–04:00) allows the ETVs to fully recharge for the next day. In the schedule for profile B most ETVs have one very long charging period during the day, rather than at night. Comparing profiles B and D in Fig. 6(a) confirms that allowing night charging leads to a substantial difference in objective value (on average 10% of the maximum objective value per fleet size).
- Last, charging profile E allows charging for every vehicle at any time. The energy demand that typically appears under these circumstances is as in Fig. 5(e): demand from 06:00–23:00 is roughly triangular shaped, with a peak between 15:00–17:00.

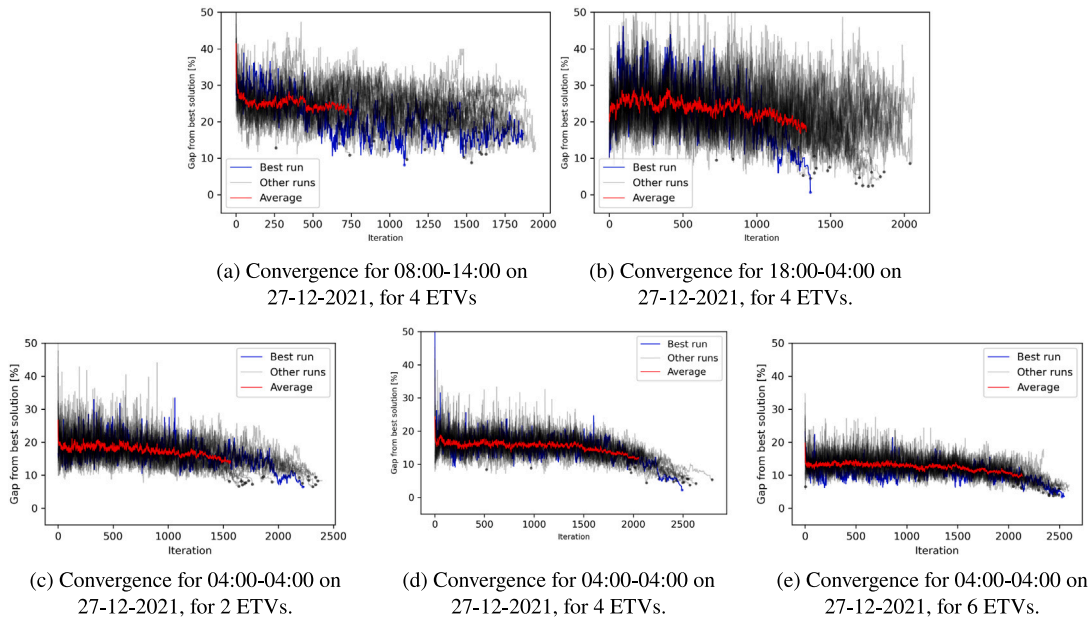


Fig. 4. Convergence of ALNS algorithm applied to various problem instances. The run attaining the largest objective value is indicated in blue, the average is indicated in red. The best result of every run is indicated by a dot in the respective colour.

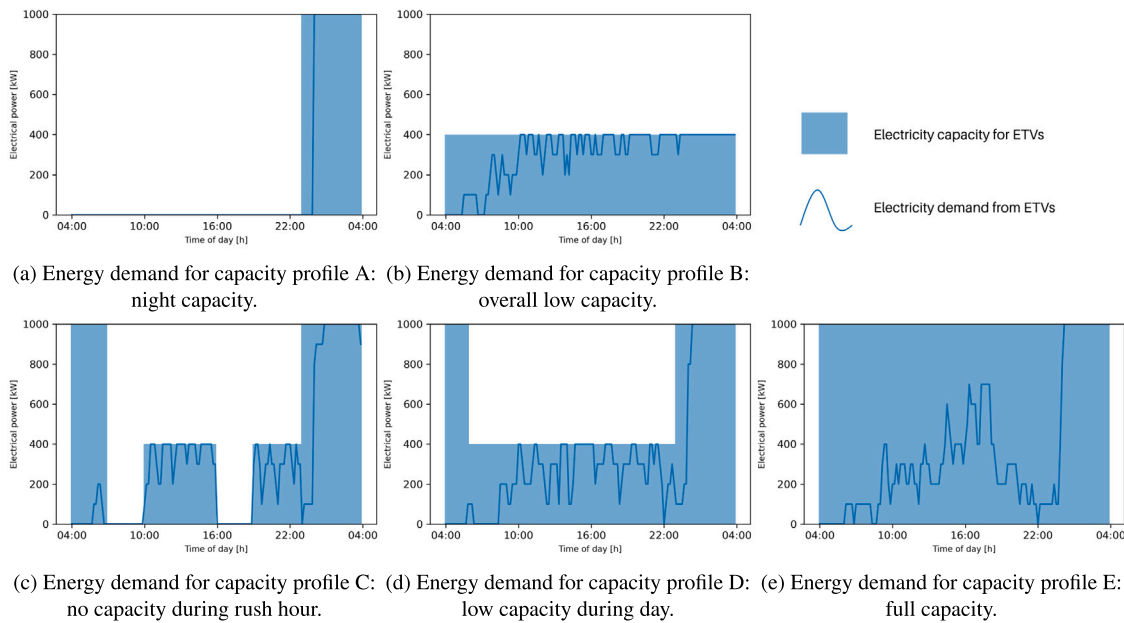


Fig. 5. The electrical power available during the day, for the five energy profiles considered. For every profile, the energy demand per time step associated with an ETV schedule generated using the ALNS model. The fleet size is ten ETVs, and the time period is 04:00–04:00 on 27-12-2021.

Upon examination of the optimized schedules, we find two types of ETVs in the schedule: one with a long charging period near 15:00–17:00, that needs no other charging before the night. The other type is charged for 3 or 4 shorter periods, spread out during the day. Together this forms a triangular shaped demand.

In addition, it is interesting to investigate the *marginal capacity benefit*: the benefit for an airport of providing one more charging position (i.e. increase capacity by P^c kW) for the total towing time in the optimized ETV schedule. This benefit can be weighed against the costs of a new charging position.

Fig. 6(b) shows the results of applying the ALNS model with various equidistant values of electricity capacity. The electricity capacity is assumed to be constant over the entire day. Every newly added charging

position contributes less to the objective value than the previous one. The figure suggests that after 12 charging positions (in this case 60% of the fleet size), the improvement stagnates. The limit for the ETV fleet with the current characteristics is roughly 2500 towed km (273 ton CO_2). The same analysis can be performed for different capacity profiles and fleet sizes.

6.3. Impact of fast charging and battery size on ETV fleet utilization

Throughout the previous sections, the charging rate P^c and battery capacity Q have remained constant. The values chosen are considered realistic for application at the time of writing. However, given their large influence on the ETV schedules resulting from the models,

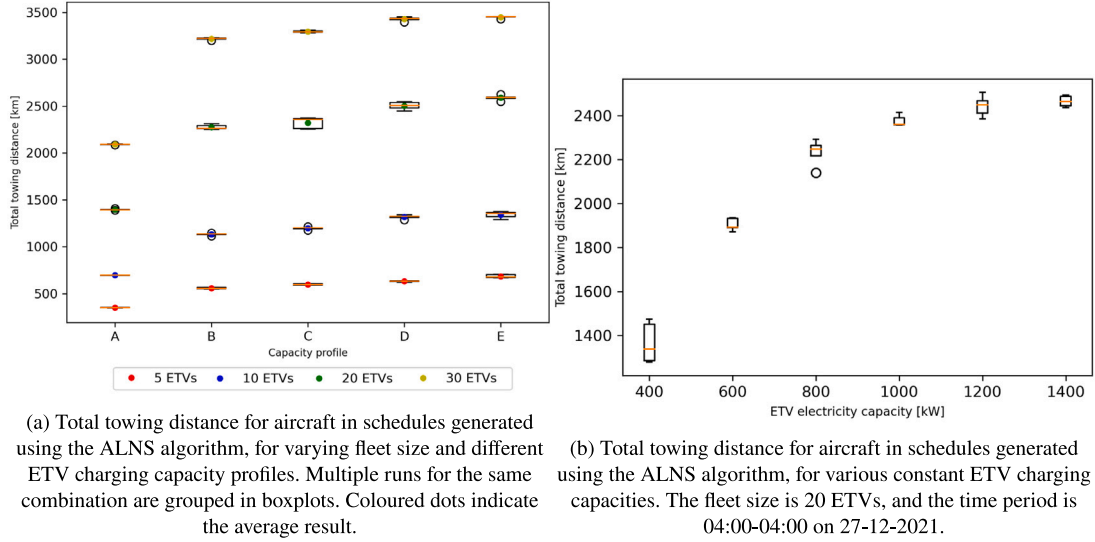


Fig. 6. Total towing distance in km (Eq. (28)) of schedules generated with the ALNS algorithm, for various model settings, during 04:00–04:00 on 27-12-2021.

Table 4

Impact of fast charging and ETV battery capacity; charging rate $P^c \in \{50, 100, 150, 200\}$ kW and battery capacity $Q \in \{200, 400, 600\}$ kWh. The total towing distance in km (Eq. (28)) obtained in schedules created with the ALNS algorithm.

	P^c			
	50 kW	100 kW	150 kW	200 kW
Q				
200 kWh	1846.8 ± 12.5	2183.0 ± 36.9	2283.6 ± 39.1	2407.4 ± 26.5
400 kWh	1942.1 ± 20.5	2508.6 ± 18.8	2608.8 ± 21.3	2713.3 ± 8.7
600 kWh	1940.9 ± 29.6	2634.7 ± 30.8	2731.0 ± 77.6	2797.8 ± 16.6

it is instructive to consider (combinations of) other values of these parameters.

Table 4 shows the total towed distance obtained when varying the charging rate and battery capacity. The average and standard deviation of 5 runs are shown for every combination. The fleet size is 20 and the electricity capacity is given by profile D. The average runtime is 134 min. Note that we assume constant towing and driving power P^X and P^S . In actuality, increasing the battery capacity will increase these values, due to the ETV becoming heavier.

From the table we deduce that if the charging rate is as small as 50 kW, increasing the battery size from 200 kWh will provide little benefits. At this charging rate, the utilization time of the ETVs is up to 25% smaller than for charging rates of 100 kW and over. There, the increase of objective value with increasing battery size is also considerably larger. The generated schedules show that for $P^c = 50$ kW the ETVs spend up to half the day charging, and the ETVs rarely use more than 300 kWh of their battery.

We observe that at any battery capacity, increasing the charging rate leads to significant increases in objective value. This is mainly because the necessary charging periods during daytime can become shorter, leaving more time to tow more aircraft. The time taken up by charging during the day is inversely proportional to P^c . Therefore, the increases in objective value become smaller with each increase of P^c . Note that the electricity capacity does not grow with the charging rate; if the capacity is 800 kW, then 8 ETVs can charge when $P^c = 100$ kW, and 4 ETVs can charge when $P^c = 200$ kW.

For values in the top right of Table 4, an ETV is recharged the fastest; as fast as 1 h. This makes the window for allowed charging periods rather small, since there is also a minimum charging time of 30 min. Given an intermediate solution, the ALNS algorithm may not find a legal move for charging periods when adding or removing aircraft. This results in solutions where many ETVs tow far fewer aircraft than optimal. For $t_{\min}^C = 30$ min the results for $Q = 200$ kWh

and $P^c = 200$ kW are 1771.6 ± 136.5 km. A solution is to allow a smaller minimum charging time for this combination, which is fitting for a situation with fast charging. The results in Table 4 for this combination are obtained using $t_{\min}^C = 20$ min.

From the optimized schedules summarized in the table, and the observations above, we can deduct a relation between the objective value and P^c and Q . We observe:

- In almost all cases, the time available for night charging (00:00–04:00) is fully used, unless a full charge takes less than 4 h. Between 04:00 and 06:00 there are very few flights and no charging.
- Any charging during the rest of the day (06:00–00:00) prevents ETVs from towing aircraft. The sum of the time spent charging during the day and the time spent towing aircraft should equal 18 h.
- It is assumed that at any point in time, the supply of aircraft that can be towed outstrips the towing potential of the ETV fleet size.

An approximation for the total towed distance, in the case where day charging is necessary, is then derived as follows:

$$t^d = t_C^d + t_X^d = \frac{q_{\text{km}} d_{\text{tot}}^X - q^{\text{night}}}{P^c} + t_{\text{km}}^{\text{ETV}} d_{\text{tot}}^X, \quad (60)$$

so that

$$d_{\text{tot}}^X = \frac{\frac{q^{\text{night}}}{P^c} + t^d}{t_{\text{km}}^{\text{ETV}} + \frac{q_{\text{km}}}{P^c}}. \quad (61)$$

Here t^d is the total daytime available to the fleet in hours, i.e. $t^d = 18N^V$, t_C^d and t_X^d are the total daytime spent charging and towing, respectively, q_{km} is the average energy needed per km towing, d_{tot}^X is the total towed distance in the schedule, q^{night} is the total energy that can be charged during the night and $t_{\text{km}}^{\text{ETV}}$ is the average time spent by an ETV towing an aircraft for one km.

These expressions are found as:

$$q^{\text{night}} = N^V P^c \min\left\{\frac{Q}{P^c}, 4\right\}, \quad (62)$$

$$q_{\text{km}} = \frac{\sum_{a \in A} q^X(a)}{\sum_{a \in A} d_a^X} \quad (63)$$

Last, $t_{\text{km}}^{\text{ETV}}$ is found by considering the runs forming Table 4, dividing the total time not used for charging by the total towed distance.

In case no day charging is necessary, the expression (61) reduces to:

$$d_{\text{tot}}^X = \frac{I^d}{k_{\text{ETV}}} \quad (64)$$

By using these formulae all values obtained experimentally in Table 4 and the values for profile D in Fig. 6(a) are approximated to within 6%. The approximation slightly overestimates the objective values for smaller values of Q , and slightly underestimates them for larger values of Q . A possible explanation is that there is a benefit that comes with a larger Q , that is not factored in with this approximation: an ETV with larger battery capacity will less often reach a SOC of 0, which would leave a time gap without towing until its next charging opportunity.

The approximation given in Eqs. (60)–(64) can be further extended to allow for variation in ETV capacity profile and towing power P^X . It can also be altered to adhere to a different charging strategy, for example, if one would relax the restriction of ending the day with full battery capacity. The model can be used by airport planners to gauge the emission reductions associated with acquiring an ETV fleet with any values of Q , P^c or N^V . For example, one can weigh the added costs of using very fast charging technology against the expected environmental benefits. With the current settings, a fast charging system that provides 500 kW per charging point can provide another 7% increase in towed distance for $Q = 200$ kWh. For larger Q this advantage shrinks. For $Q = 750$ kWh night charging suffices from $P^c = 150$ kW onwards, and very fast charging becomes unnecessary. Eq (64) suggests a maximum objective value of 2849 km towed distance (311 ton CO₂ saved) for a fleet size of $N^V = 20$.

7. Conclusions

In this paper, two models are proposed to create schedules for electric towing and charging of a fleet of ETVs on an airport. Both models aim to maximize the total towed distance, given a flight schedule, an airport layout, an ETV fleet size, an ETV energy spending and charging model, and an airport electricity capacity profile for charging ETVs. The resulting schedules define which ETV is charging where and for how long, and which ETV is towing an aircraft, or travelling to and from a task.

The first model is an MILP model. An optimal solution or near best bound is found within several hours for instances with small fleet size and a scheduling time period of under ten hours. The goal is to find solutions for a 24 h period and fleet sizes of up to 30 vehicles. Therefore, the second model uses ALNS, combined with Simulated Annealing and Tabu Search. We have seen that this heuristic model can consistently find solutions with an optimality gap of an average of 4% percent for the smaller instances, and can solve the NP-hard large instances, which cannot be solved using the MILP solver, in several hours. Therefore, we conclude that it is possible to pursue optimization of ETV-to-aircraft assignment for a large fleet within a few hours, making the problem tractable. The removal and insertion heuristics introduced to move between different solutions vary in performance: the best heuristics are random removal/insertion, vehicle removal, cluster removal, and greedy insertion. These heuristics work best to improve the towed distance, and thus the utilization of the towing vehicles.

In order to investigate the effects of operating in a period with limited electricity capacity at the airport, the ALNS model was applied to a full day of operations at Amsterdam Airport Schiphol, with five different ETV electricity capacity profiles. For the battery and ETV properties assumed in this work, it was found that charging at night (when there are no aircraft to tow) is necessary to fulfil the potential of the ETV fleet, but not sufficient to tow all aircraft, leading to a performance of 54% of the performance without capacity restrictions. Charging capacity during the day is therefore crucial to improve ETV utilization time. The results show that even with only small intermittent

periods of no charging, the best solution will contain time periods with fewer or shorter tasks than can potentially be scheduled. The average performance difference between day charging (profile D) and no capacity during rush hour (profile C) is 6.4%. Last, when charging is allowed for any ETV at any time of day, the ETV daily electricity demand generally forms a triangle shape, placing the largest demand on the electricity network at 15:00–17:00.

The effects of airport investments in ETV battery capacity and fast charging technology on the environmental benefits of the ETV fleet have been explored. A relation between the total towed distance and these parameters was derived from observations. It was found that charging slower than 100 kW will reduce the total towed distance to well below the potential of the ETV fleet. Faster charging will improve the towed distance by freeing time during the day to tow more aircraft, but with diminishing returns. For battery capacities higher than 750 kWh, all necessary charging can be done at night, and very fast charging becomes unnecessary. Under such circumstances, a fleet of 20 ETVs could prevent the emissions of 311 ton CO₂ per day at the airport. With realistic battery characteristics and limited daytime electricity capacity, the saved emissions still amount to 274 ton CO₂.

The models introduced in this paper can be applied to other airports and flight schedules, with their own potential ETV electricity capacity profiles. The results can be used to decide when and whether to implement electric taxiing at the airport, and if so, with how many charging points and ETVs. Or, when such a system is already in place, to consider the costs and benefits of increasing the fleet size, or the amount of charging locations, given the current and future charging capacity.

Future work includes optimizing real-time operations of an airport with a fleet of ETVs, including disruptions such as flight delays and cancellations and ETV unavailability. Such a continuous solution process, that could be based on creating schedules in a rolling horizon approach, would aim to maximize emission reduction and robustness. It would constitute the next step in integrating ETV fleet scheduling optimization into actual airport operations. Another upcoming research area is the development of autonomous airport surface movement, including for ETVs.

CRedit authorship contribution statement

M. Zoutendijk: Conceptualization, Investigation, Formal analysis, Methodology, Visualization, Writing – original draft, Writing – review & editing. **M. Mitici:** Conceptualization, Methodology, Writing – original draft, Writing – review & editing.

Declaration of competing interest

The authors declare that they have no known competing financial interests or personal relationships that could have appeared to influence the work reported in this paper.

Data availability

The authors do not have permission to share data.

Appendix. Glossary

All abbreviations and notation used throughout the paper are gathered in Table A.1 for reference.

Table A.1
Glossary of notation and abbreviations.

Abbreviation or symbol	Explanation
Airport representation	
$G^X = (N^X, E^X)$	Taxiway network
$G^S = (N^S, E^S)$	Service road network
v^s, v^x	Speed on service roads/taxiways
$n_{cs,i}, N_{cs}$	Charging station i , number of charging stations
n_{dp}	ETV depot node
Aircraft routing	
$T = [t^s, t^e]$	Scheduling time interval
N^T, Δ	Number of time steps, step size
$N^{F,S}, N^F$	Number of flight movements during P without/with artificial aircraft
$A = A^S \cup A^e$	Set of aircraft (nonartificial + artificial)
$d^X(m, n), d^S(m, n)$	Distance over taxiway network/service road network from m to n
t_a^p, t_a^d	Pick-up and drop-off time of aircraft a
n_a^p, n_a^d	Pick-up and drop-off node of aircraft a
t_{sep}	Separation time
ETVs	
Electric Towing Vehicles	
N^V	ETV fleet size
P^c, P^X, P^S	Charging rate, towing power, driving power
Q	Battery capacity
t_{min}^c	Minimum charging time
t^c	Connecting/Disconnecting time
$t^c(a, b)$	Time available between towing consecutive aircraft a and b
$q^X(a)$	Energy needed to tow aircraft a
$q^S(n, m)$	Energy needed to travel from node n to m
$q^S(a, b), q^C(a, b)$	Energy needed to travel from n_a^d to n_b^p /from n_a^d to n_b^p via a $n_{cs,i}$
$q_a^S(a)$	Energy needed to travel from n_{dp} to n_a^p
$q_1^C(a), q_2^C(a)$	Energy needed to travel from the closest $n_{cs,i}$ to n_a^p /from n_a^d to the closest $n_{cs,i}$
MILP model	
Mixed Integer Linear Programming model	
A_a^{out}, A_a^{in}	Set of aircraft that can be towed by an ETV after/before it tows aircraft a
A_a^{PC}	Set of aircraft in A_a^{out} for which there is at least t_{min}^c time for effective charging
v_a	Vehicle that tows aircraft a
x_{ab}	Variable indicating if a and b are towed consecutively
x_a^f, x_a^l	Indicates if a is the first/last aircraft an ETV tows
q_a	Indicates state of charge of ETV at the start of towing a
c_a	Indicates if ETV is charged after towing aircraft a
c_a^t, c_a^s	Indicates charging time/start time of charging of ETV
α_{at}, β_{at}	Indicates if charging of ETV v_a starts earlier/finishes later than time step t
γ_{at}	Indicates if ETV v_a is charged during time step t
y_a	Indicates if a is towed by an ETV or taxis by itself
ALNS	
Adaptive Large Neighbourhood Search	
$s, f(s), s^{all}$	Solution and its objective value, set of all solutions
s^l, s^c, s^l, s^b	Initial, candidate, last and best solution
$\pi_{i,j}^-, \pi_{i,j}^+$	Removal and insertion selection scores for heuristic i and segment j
$\bar{\pi}_{i,j}^-, \bar{\pi}_{i,j}^+$	Removal and insertion segment selection scores for heuristic i and segment j
$a_{i,j}^-, a_{i,j}^+$	Selection rate during segment j of removal/insertion heuristic i
N^{it}	Number of ALNS iterations
N^{seg}	Number of iterations in ALNS segment
N^{rem}	Number of aircraft removed in heuristic
A^{rem}, A_v^{ins}	Set of aircraft removable from the schedule/insertable in the schedule of ETV v
Simulated Annealing	
$\sigma_1, \sigma_2, \sigma_3$	Global, previous and accepted solution reward
ρ	Reaction factor
w	Start temperature control parameter
c	Cooling rate

References

[1] Federal Aviation Administration. Aviation climate action plan. 2021, URL: https://www.faa.gov/sites/faa.gov/files/2021-11/Aviation_Climate_Action_Plan.pdf.

[2] European Commission. Reducing emissions from aviation. 2021, URL: https://ec.europa.eu/clima/eu-action/transport-emissions/reducing-emissions-aviation_en.

[3] Smart Airport Systems. Taxibot international. 2022, URL: <https://www.taxibot-international.com/>.

[4] Schiphol. The benefits of sustainable taxiing. 2021, URL: <https://www.schiphol.nl/en/innovation/page/the-benefits-of-sustainable-taxiing/>.

[5] Guo R, Zhang Y, Wang Q. Comparison of emerging ground propulsion systems for electrified aircraft taxi operations. *Transp Res C* 2014;44:98–109.

[6] Hein K, Baumann S. Acoustical comparison of conventional taxiing and dispatch towing - Taxibot's contribution to ground noise abatement. In: 30th congress of the international council of the aeronautical sciences. ICAS, 2016, p. 1–7.

[7] Bunte S, Klierer N. An overview on vehicle scheduling models. *Public Transp* 2009;1(4):299–317.

[8] Hoff A, Andersson H, Christiansen M, Hasle G, Løkketangen A. Industrial aspects and literature survey: Fleet composition and routing. *Comput Oper Res* 2010;37(12):2041–61, URL: <http://dx.doi.org/10.1016/j.cor.2010.03.015>.

[9] Rahman HF, Nielsen I. Scheduling automated transport vehicles for material distribution systems. *Appl Soft Comput* 2019;82:105552, URL: <https://doi.org/10.1016/j.asoc.2019.105552>.

[10] Alizadeh Foroutan R, Rezaeian J, Mahdavi I. Green vehicle routing and scheduling problem with heterogeneous fleet including reverse logistics in the form of collecting returned goods. *Appl Soft Comput* 2020;94:106462, URL: <https://doi.org/10.1016/j.asoc.2020.106462>.

[11] Ganji M, Kazemipoor H, Hadji Molana SM, Sajadi SM. A green multi-objective integrated scheduling of production and distribution with heterogeneous fleet vehicle routing and time windows. *J Clean Prod* 2020;259:120824, URL: <https://doi.org/10.1016/j.jclepro.2020.120824>.

- [12] Andrade-Michel A, Ríos-Solís YA, Boyer V. Vehicle and reliable driver scheduling for public bus transportation systems. *Transp Res B* 2021;145:290–301, URL: <https://doi.org/10.1016/j.trb.2021.01.011>.
- [13] Hiermann G, Puchinger J, Ropke S, Hartl RF. The electric fleet size and mix vehicle routing problem with time windows and recharging stations. *European J Oper Res* 2016;252(3):995–1018.
- [14] Schiffer M, Walther G. The electric location routing problem with time windows and partial recharging. *European J Oper Res* 2017;260(3):995–1013.
- [15] Keskin M, Çatay B. Partial recharge strategies for the electric vehicle routing problem with time windows. *Transp Res C* 2016;65:111–27.
- [16] Emde S, Abedinnia H, Glock CH. Scheduling electric vehicles making milk-runs for just-in-time delivery. *IIE Trans* 2018;50(11):1013–25.
- [17] Frey CM, Jungwirth A, Frey M, Kolisch R. The vehicle routing problem with time windows and flexible delivery locations. *European J Oper Res* 2023;308(3):1142–59.
- [18] Foda A, Abdelaty H, Mohamed M, El-Saadany E. A generic cost-utility-emission optimization for electric bus transit infrastructure planning and charging scheduling. *Energy* 2023;277(April):127592.
- [19] van Baaren E, Roling PC. Design of a zero emission aircraft towing system. In: *AIAA AVIATION forum*. 2019, p. 1–11.
- [20] Soltani M, Ahmadi S, Akgunduz A, Bhuiyan N. An eco-friendly aircraft taxiing approach with collision and conflict avoidance. *Transp Res C* 2020;121(December 2019):102872.
- [21] Salihu AL, Lloyd SM, Akgunduz A. Electrification of airport taxiway operations: A simulation framework for analyzing congestion and cost. *Transp Res D* 2021;97(July).
- [22] Zaninotto S, Gauci J, Zammit B. Tow truck taxi algorithm: An engineless taxi operations system using battery-operated autonomous tow trucks. In: *33rd congress of the international council of the aeronautical sciences*. 2022, p. 1–18.
- [23] van Oosterom S, Mitici M, Hoekstra J. Dispatching a fleet of electric towing vehicles for aircraft taxiing with conflict avoidance and efficient battery charging. *Transp Res C* 2023;147(January).
- [24] Ahmadi S, Akgunduz A. Airport operations with electric-powered towing alternatives under stochastic conditions. *J Air Transp Manag* 2023;109(January):102392.
- [25] European Commission. Zero emission vehicles: first 'Fit for 55' deal will end the sale of new CO2 emitting cars in Europe by 2035. 2022, URL: https://ec.europa.eu/commission/presscorner/detail/en/ip_22_6462.
- [26] Mahmud K, Hossain MJ, Ravishankar J. Peak-load management in commercial systems with electric vehicles. *IEEE Syst J* 2019;13(2):1872–82.
- [27] Li X, Tan Y, Liu X, Liao Q, Sun B, Cao G, Li C, Yang X, Wang Z. A cost-benefit analysis of V2G electric vehicles supporting peak shaving in Shanghai. *Electr Power Syst Res* 2020;179(September 2019):106058.
- [28] Uddin M, Romlie MF, Abdullah MF, Abd Halim S, Abu Bakar AH, Chia Kwang T. A review on peak load shaving strategies. *Renew Sustain Energy Rev* 2018;82:3323–32.
- [29] Adegbohun F, von Jouanne A, Lee KY. Autonomous battery swapping system and methodologies of electric vehicles. *Energies* 2019;12(4):1–14.
- [30] Wu J, Su H, Meng J, Lin M. Electric vehicle charging scheduling considering infrastructure constraints. *Energy* 2023;278(February).
- [31] Forrest KE, Tarroja B, Zhang L, Shaffer B, Samuelsen S. Charging a renewable future: The impact of electric vehicle charging intelligence on energy storage requirements to meet renewable portfolio standards. *J Power Sources* 2016;336:63–74.
- [32] Moon HB, Park SY, Jeong C, Lee J. Forecasting electricity demand of electric vehicles by analyzing consumers' charging patterns. *Transp Res D* 2018;62(February):64–79.
- [33] Ortega Alba S, Manana M. Energy research in airports: A review. *Energies* 2016;9(5):1–19.
- [34] Uysal MP, Sogut MZ. An integrated research for architecture-based energy management in sustainable airports. *Energy* 2017;140:1387–97.
- [35] Ortega Alba S, Manana M. Characterization and analysis of energy demand patterns in airports. *Energies* 2017;10(1):1–35.
- [36] Gulan K, Cotilla-Sanchez E, Cao Y. Charging analysis of ground support vehicles in an electrified airport. In: *IEEE transportation electrification conference. ITEC*, 2019, p. 1–6.
- [37] Doctor F, Budd T, Williams PD, Prescott M, Iqbal R. Modelling the effect of electric aircraft on airport operations and infrastructure. *Technol Forecast Soc Change* 2022;177:121553.
- [38] Zoutendijk M, Mitici M, Hoekstra J. An investigation of operational management solutions and challenges for electric taxiing of aircraft. *Res Transp Bus Manag* 2023;49(January):101019.
- [39] Deonandan I, Balakrishnan H. Evaluation of strategies for reducing taxi-out emissions at airports. In: *10th AIAA aviation technology, integration and operations (ATIO) conference*. Vol. 3, 2010, p. 1–14.
- [40] Dzikus N, Fuchte J, Lau A, Gollnick V. Potential for fuel reduction through electric taxiing. In: *11th AIAA aviation technology, integration, and operations (ATIO) conference*. 2011, p. 1–9.
- [41] Zhang M, Huang Q, Liu S, Li H. Assessment method of fuel consumption and emissions of aircraft during taxiing on airport surface under given meteorological conditions. *Sustainability (Switzerland)* 2019;11(21).
- [42] Nojumi H, Dincer I, Naterer GF. Greenhouse gas emissions assessment of hydrogen and kerosene-fueled aircraft propulsion. *Int J Hydrogen Energy* 2009;34(3):1363–9.
- [43] Schiphol Group. Schiphol developer center. 2022, URL: <https://developer.schiphol.nl/login>.
- [44] Scarlat N, Prussi M, Padella M. Quantification of the carbon intensity of electricity produced and used in Europe. *Appl Energy* 2022;305:117901.
- [45] Kollmuss A. Carbon offsetting & air travel: Part 1: CO2-emissions calculations. Technical report, Stockholm Environment Institute; 2008, URL: https://mediamanager.sei.org/documents/Publications/Climate/sei_air_travel_emissions_paper1_27_03_09.pdf.
- [46] Zoutendijk M, van Oosterom S, Mitici M. Electric taxiing with disruption management: Assignment of electric towing vehicles to aircraft. In: *AIAA aviation forum* 2023. 2023, p. 1–20.
- [47] Ropke S, Pisinger D. An adaptive large neighborhood search heuristic for the pickup and delivery problem with time windows. *Transp Sci* 2006;40(4):455–72.
- [48] Pisinger D, Ropke S. A general heuristic for vehicle routing problems. *Comput Oper Res* 2007;34(8):2403–35.
- [49] Kirkpatrick S, Gelatt Jr CD, Vecchi MP. Optimization by simulated annealing. *Science* 1983;220(4598):671–80.
- [50] Glover F. Future paths for integer programming and links to artificial intelligence. *Comput Oper Res* 1986;13(5):533–49.
- [51] Luchtverkeersleiding Nederland. Runway use. 2022, URL: <https://en.lvn.nl/environment/runway-use>.
- [52] van Oosterom S, Mitici M, Hoekstra J. Analyzing the impact of battery capacity and charging protocols on the dispatchment of electric towing vehicles at a large airport. In: *AIAA aviation forum* 2022. 2022, p. 1–11.
- [53] Schiphol. Schiphol regulations. Technical report, Amsterdam Airport Schiphol; 2022, URL: <https://www.schiphol.nl/en/download/1609745377/43q9kGoE92CcmEeC6awa4.pdf>.
- [54] Munich International Airport. Traffic and Safety Rules: for the non-public area at Munich Airport. Technical report, Munich International Airport; 2016, p. 8, URL: https://www.munich-airport.de/_b/000000000000008368639b5e302e6f/traffic-safety-rules-2016.pdf.
- [55] Schiphol. Sustainable taxiing and the Taxibot. 2020, URL: <https://www.schiphol.nl/en/download/b2b/1594319068/40LYaERw5x8BuRuXpVQkik.pdf>.